

Collective spin and orbital excitations in a canonical orbital system KCuF_3

Jiemin Li,^{1,2} Lei Xu,^{3,*} Mirian Garcia-Fernandez,¹ Abhishek Nag,¹ H. C. Robarts,^{1,4} A. C. Walters,¹ X. Liu,⁵ Jianshi Zhou,⁶ Krzysztof Wohlfeld,⁷ Jeroen van den Brink,^{3,8} Hong Ding,² and Ke-Jin Zhou^{1,†}

¹*Diamond Light Source, Harwell Campus, Didcot OX11 0DE, United Kingdom*

²*Beijing National Laboratory for Condensed Matter Physics and Institute of Physics, Chinese Academy of Sciences, Beijing 100190, China*

³*Institute for Theoretical Solid State Physics, IFW Dresden, Helmholtzstrasse 20, D-01069 Dresden, Germany*

⁴*H. H. Wills Physics Laboratory, University of Bristol, Bristol BS8 1TL, United Kingdom*

⁵*School of Physical Science and Technology, ShanghaiTech University, Shanghai 201210, China*

⁶*The Materials Science and Engineering Program, Mechanical Engineering, University of Texas at Austin, Austin, Texas 78712, USA*

⁷*Institute of Theoretical Physics, Faculty of Physics, University of Warsaw, Pasteura 5, PL-02093 Warsaw, Poland*

⁸*Institut für Theoretische Physik and Würzburg-Dresden Cluster of Excellence ct.qmat, Technische Universität Dresden, 01062 Dresden, Germany*

(Dated: 2020/10/26)

We study the collective spin and orbital excitations in the canonical orbital system KCuF_3 . Using the Cu L_3 -edge resonant inelastic X-ray scattering we show that the non-dispersive high-energy peaks result from the Cu^{2+} dd orbital excitations. These high-energy modes show good agreement with the *ab-initio* quantum chemistry calculation based on a single cluster, indicating that the dd excitations are highly localized. At the same time, the low-energy excitations present clear dispersion. They match extremely well with the two-spinon continuum following the comparison with Mueller Ansatz calculations. The localized dd excitations and the observation of the strongly dispersive magnetic excitations suggest that orbiton dispersion is below the resolution detection limit. Our results can reconcile with the strong *local* Jahn-Teller effect in KCuF_3 , which predominantly drives orbital ordering.

I. INTRODUCTION

In strongly correlated quantum materials, the coupling between orbital and charge, spin or lattice degrees of freedom often leads to many fascinating phenomena [1]. For example, the colossal magnetoresistive manganese perovskites display striking changes in resistivity under a moderate magnetic field. These unusual transport properties appear to be connected with strong spin order and orbital order coupling [2]. In YVO_3 , it was reported that the multiple temperature-induced magnetization reversals may be related to a change in orbital ordering [3]. As one of few pseudocubic perovskite systems, KCuF_3 possesses unusual three-dimensional (3D) orbital physics and quasi-one-dimensional (1D) magnetic properties [4, 5]. Owing to cooperative Jahn-Teller (JT) distortions of CuF_6 octahedra, the ground state of KCuF_3 hole orbitals $d_{x^2-z^2}$ and $d_{y^2-z^2}$ alternates in all crystalline directions. As such, strong superexchange interaction is developed along the c -axis, while in the ab plane exchange interactions are significantly smaller irrespective of the pseudocubic crystal structure. It was reported that the Cu $3d$ orbitals form long-range orbital order (OO) at very high temperature of about 800 K and the system undergoes a 3D antiferromagnetic (AFM) ordering below T_N of 38 K [4, 6, 7]. The underlying mechanism has been an

interesting subject but it is generally accepted that OO is largely driven by the JT effect [8].

In principle, one of the main signatures of the presence of the OO phase in a correlated compound, is the onset of a concomitant collective orbital excitation - orbiton. The latter is best identified by its characteristic dispersion relation which is traditionally understood as stemming from the so-called superexchange coupling [9], *i.e.*, a remnant of the electronic motion in the Mott insulators with mobile spin and/or orbital degrees of freedom but frozen charge. On the theoretical side, one of the best studied cases is the nicely dispersing orbiton in the ferromagnetic plane of LaMnO_3 [10]. Unfortunately, despite initial positive reports [11], such a proposal has not been experimentally verified [12], possibly due to the lack of the proper experimental probes in the past and/or complex multiplet structure of the manganese ions of a hypothetical RIXS experiment. It was then only the experimental observation of a large orbiton dispersion in three distinct quasi-1D cuprates that has found its explanation in the superexchange mechanism [13–15]. Crucially, the latter is possible *despite* the strong coupling between orbitons and the magnetic excitations (spinons) in these quasi-1D antiferromagnets with ferroorbital order [16, 17], suggesting that the antiferromagnetic correlations along the c axis of LaMnO_3 should not *a priori* hinder the observation of an orbiton. Altogether, the above discussion suggests that KCuF_3 , with a simple multiplet structure of the Cu^{2+} ion and a qualitatively similar orbital and magnetic order as LaMnO_3 , should be an excellent candidate for a potential observation of the orbiton.

* Present Address: Theoretical Division, Los Alamos National Laboratory, Los Alamos, New Mexico 87544, USA

† kejin.zhou@diamond.ac.uk

Moreover, in the case of KCuF_3 , the superexchange should not be considered the only mechanism that is responsible for the orbiton dispersion. As already discussed, the OO itself is mostly driven by the JT mechanism. Since the JT Hamiltonian has an identical form to the orbital part of the superexchange one [9, 18–20], one could imagine that it should also lead to the onset of the orbiton dispersion, that is identical to the one predicted by the orbital part of the superexchange model, albeit at a much larger energy scale $\propto T_{OO} \sim 800\text{K} \gg T_N \sim 38\text{K}$ [6]. This suggests that actually an orbiton dispersion at the order of OO energy scale, i.e. $\sim 70\text{meV}$, should be observable in a RIXS experiment at the Cu L edge of KCuF_3 . Therefore, the main goal of this paper is to verify whether this is indeed possible.

In this Letter, we employ high energy-resolution resonant inelastic X-ray scattering (RIXS) to explore the orbital excitations in KCuF_3 at the Cu L_3 -edge. L -edge RIXS is well established in probing directly the dd orbital excitations as well as the collective magnetic excitations in transition metal oxides [21–23]. Particularly, RIXS is unique in probing the orbitons in systems with sizeable spin-orbital entanglement such as Sr_2CuO_3 and titanates [13, 24]. It is therefore ideal to apply RIXS to shed light on the orbital physics in KCuF_3 . At high energy, dd excitations from non-degenerated $\text{Cu}^{2+} 3d$ orbitals are resolved. They are non-dispersive in the reciprocal space but demonstrate remarkable intensity evolution. Using *ab initio* quantum chemistry calculation based on single CuF_6 cluster, dd excitations are successfully reproduced indicating that the local crystal-field splitting induced by a JT distortion dominates the high-energy dd excitations rather than the collective orbitons. At the low energy range dispersive excitations are clearly resolved. Through Muller Ansatz calculations, we conclude the dispersive excitations in the low-energy are dominated by the two-spinon continuum. Our results suggest that orbitons, if they exist, may appear at much lower energy scale than the energy resolution.

II. EXPERIMENTAL DETAILS

Single crystal KCuF_3 compounds were prepared by the method described in Ref.[25]. A pristine sample with the surface normal $(0\ 0\ 1)$ was selected and characterized by a lab-based Laue diffractometer prior to the RIXS measurements. We confirm the sample has the type- a orbital order structure [26]. The RIXS experiments were conducted at the I21-RIXS beamline at Diamond Light Source, United Kingdom. The sample was mounted with the $(1\ 1\ 0)$ plane lying in the scattering plane, shown in Fig.1 (b). The 2θ scattering angle was fixed at 146° throughout the experiment. The measuring temperature was kept at 16 K unless stated otherwise. We tuned the incident photon energy to the resonance of the Cu L_3 absorption peak (see Fig.1 (a)) with either linear-horizontal (σ) or linear-vertical (π) polarizations for RIXS measurements. RIXS signals were collected without polarization analysis. For all RIXS spectra, the elastic (zero-energy

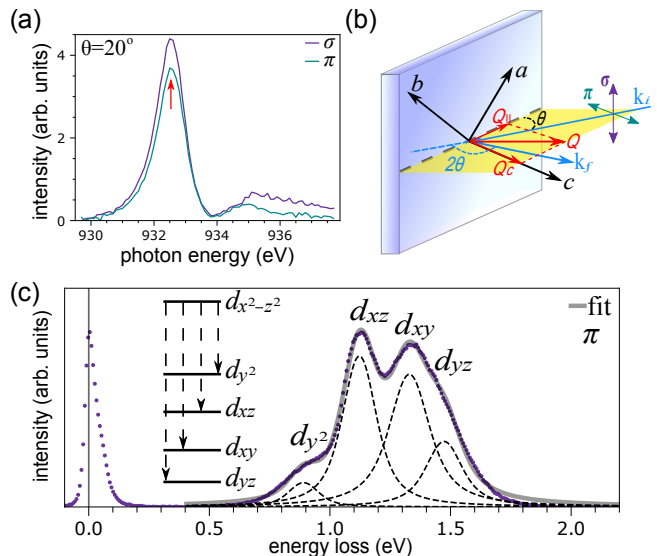


FIG. 1. (a) Cu L_3 -XAS spectra of KCuF_3 collected with the partial fluorescence yield. (b) A sketch of the experimental geometry. Light blue arrows represent the incident (k_i) and scattered (k_f) X-rays, while the double arrows (green: π , purple: σ) are for the polarizations of incident X-rays. Red arrows indicate the momentum transfer and the corresponding projection parallel and perpendicular to the sample surface. Crystal axes are represented by black arrows. (c) A fitting example of the dd excitations. The purple dotted line is an experimental spectrum and the grey solid line represents the total fit. The inset depicts the energy splitting of $3d$ orbitals.

loss) peak positions were determined by the elastic scattering spectrum from carbon tape near the sample surface and then fine adjusted by the Gaussian fitted elastic peak position. All RIXS spectra are normalized by the integrated intensities from the high energy region (0.5 eV \sim 2 eV). The Miller indices in this study are defined by a pseudo-tetragonal unit cell with $a = b \simeq 4.146\text{ \AA}$ and $c \simeq 3.92\text{ \AA}$. The momentum transfer \mathbf{q} is defined in reciprocal lattice units (r.l.u.) as $\mathbf{q} = h\mathbf{a}^* + k\mathbf{b}^* + l\mathbf{c}^*$ where $\mathbf{a}^* = 2\pi/a$, etc.

III. RESULTS AND DISCUSSION

Fig.1 (a) shows the Cu L_3 -edge X-ray absorption spectra (XAS) of KCuF_3 excited by two linear polarizations. The main peak at 932.5 eV corresponds to the $2p^53d^{10}$ final state and the shoulder peak at about 935 eV stems from the $2p^53d^{10}\underline{L}$ state (\underline{L} represents a hole at ligand- F site) [27]. The comparable Cu L_3 -edge XAS intensity demonstrates the 3D character of the orbital ground state. A representative RIXS spectrum excited by π polarized X-rays is shown in Fig.1 (c) which comprises two regions: a high-energy dd excitation which splits to four peaks, and a low-energy excitation region.

We firstly address the high-energy excitations. The energy range of dd excitations of KCuF_3 is consistent to many copper-oxides superconductors [21]. The local D_{2h} symmetry at Cu sites due to the JT distortion fully breaks

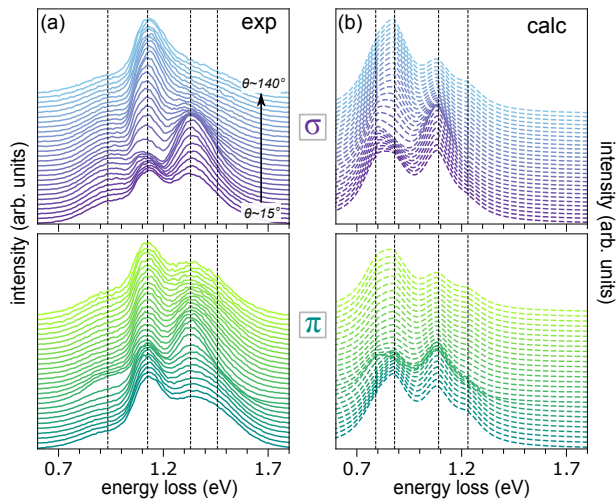


FIG. 2. (a) Angular dependence of dd excitations from σ - (purple) and π -polarized (green) incident X-rays. The vertical dashed lines depict the averaged peak values of fitted dd excitations. (c) Calculated angular-dependent spectra from the MRCI+SOC. The vertical dashed lines show the calculated values of dd excitations.

the degeneracy of Cu^{2+} $3d$ orbitals. We show the $3d$ orbitals splitting in the inset of Fig.1(c) where the ground state holds a $d_{x^2-z^2}$ hole orbital given the definition of xyz axes with respect to the crystal orientation [26]. The rotation of local distortion along each of three axes then induces the $d_{y^2-z^2}$ hole orbital at the next site, thus introducing a 3D long-range OO [28]. As demonstrated in Fig.1(c), orbital excitations are resolved to four peaks labeled with orbital character as sketched in the inset of Fig.1(c). We fitted orbital excitations with a model comprising four Lorentzian functions convoluted by Gaussian energy resolution. Together we plot the fitted dd peaks. The fitted energy positions are found to be comparable to optical and the Cu K -edge RIXS studies (see Table I in Ref. [26]) [29, 30].

To further explore the high-energy orbital excitations, we performed RIXS measurements by varying the incident θ angle from 15° to 140° . The results are shown in Fig.2(a) with the top and the bottom figures from the σ - and the π -polarizations, respectively. Assisted by the fitting analysis, we reach the conclusion that all dd excitations are non-dispersive but exhibit rich intensity variation as a function of θ . This behavior is consistent to many cuprate compounds in which dd excitations are mostly induced by the local ligand-field splitting [21].

To understand better the dd excitations, we carried out the *ab initio* Quantum Chemistry (QC) calculations using the complete active space self-consistent field (CASSCF) and multireference configuration-interaction (MRCI) as implemented in MOLPRO package [31]. An embedded cluster consisting of a single CuF_6 octahedron (one Cu atom and six F atoms, with short and long bonding lengths in *ab*-plane) was considered in the calculations, using the crystallographic data as reported in Ref. [5]. In the MRCI treatment, the F $2p$ and Cu $2s, 2p, 3s, 3p, 3d$ electrons within the single CuF_6 unit were correlated. Details

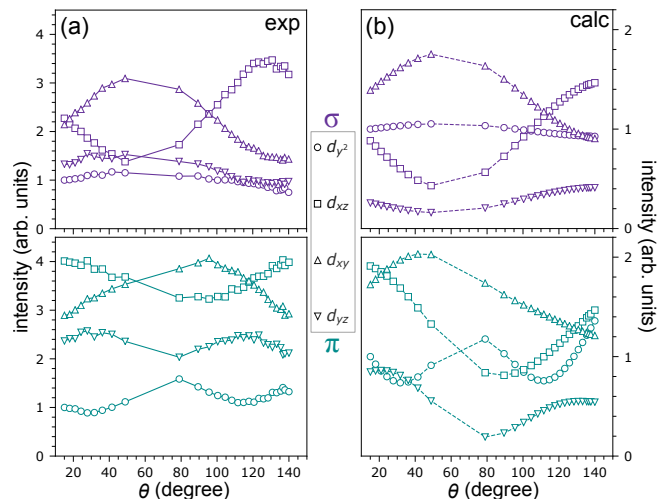


FIG. 3. Relative intensity variations as a function of θ angle for different dd excitations. (a) is the experimental results, (b) is the calculated results. The first data point of d_{y^2} orbital is normalized to a fixed intensity.

about the computed orbital excitation energies and the comparison with the experimental values are given in Ref. [26].

Fig.2 (b) shows the calculated spectra as a function of θ based on MRCI+SOC approach. The results for both polarizations agree fairly well with the experimental spectra. To compare more in detail the theory and the experimental results, we fitted all spectra and extracted the area of each orbital excitation. The intensities of each orbital excitation from the experimental and theoretical results are displayed in Fig.3(a) and Fig.3(b), respectively. The comparison shows very good agreement in terms of the trend of the angular-dependent intensity except d_{yz} orbital in the σ polarization. This discrepancy can be due to the uncertainty of determining d_{yz} intensity because of the dominating d_{xy} peak intensity. In order to take into account the orbital ordering effect, we also performed the calculation for CuF_6 octahedron rotated around c/z axis by 90° so that the hole orbital state becomes $d_{y^2-z^2}$. We then averaged the RIXS spectra from the $d_{x^2-z^2}$ and $d_{y^2-z^2}$ orbitals. It is found that the results are similar to the spectra demonstrated in Fig.2 (b) [26]. Therefore the dd excitations in KCuF_3 are strongly localized with negligible contributions from the long-range orbital ordering, in contrast to the suggestion of the existence of orbital at the high-energy range by inelastic X-ray scattering (IXS) [32].

We now turn to the discussion of the low-energy excitations. In Fig.4 (a) and (b), we display the maps of the angular-dependent low-energy excitations probed by the linear σ and π polarizations, respectively. Both maps show excitations from zero loss energy up to about 100 meV where a mode emanates from $\theta \simeq 100^\circ$ and disperses to higher energy by approaching to either side of θ range. Specifically, near θ of 80° , two maximal intensity points are present at the zero loss energy positions. In KCuF_3 , the well-known dispersive modes are the two-spinon con-

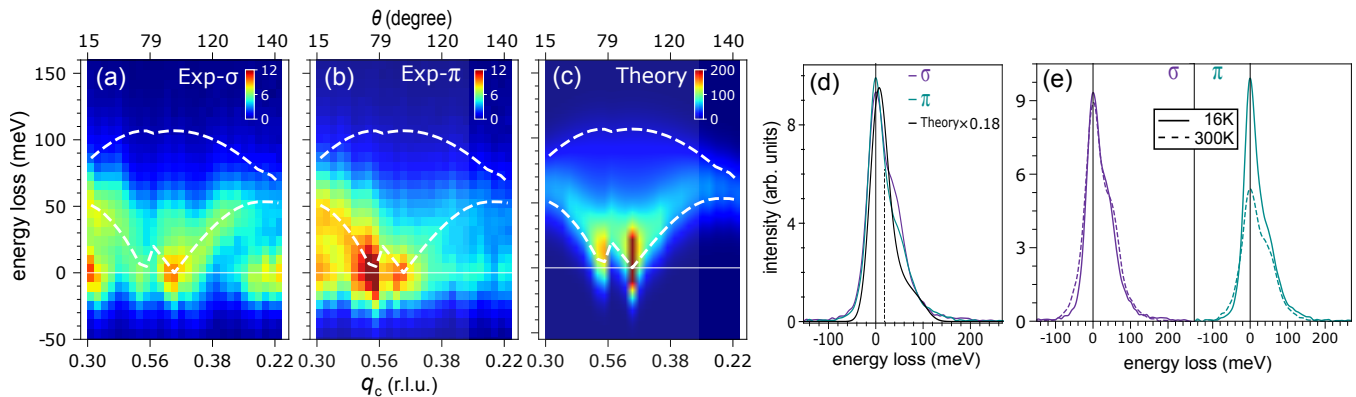


FIG. 4. (a) and (b) are color maps of the low-energy RIXS spectra from σ and π polarizations, respectively. (c) is the Muller ansatz calculated results. The white dashed lines are the lower and upper boundaries of two-spinon continuum. The thin white line is the zero energy reference. (d) The comparison of RIXS spectra at $q_c=0.5$ *r.l.u.* (e) Temperature-dependent RIXS spectra at $q_c=0.5$ *r.l.u.* for different polarizations.

tinuum reported by the inelastic neutron scattering (INS) [7]. Given the sensitivity of RIXS to magnetic excitations, we corroborate that the observed dispersive modes in RIXS are dominated by the two-spinon continuum.

To verify the assignment, we analyze more quantitatively the spin dynamics in KCuF_3 using Muller Ansatz. As established in Ref.[33], the lower and upper boundaries of the two-spinon continuum can be expressed by the following sinusoidal functions:

$$E_l(q_c) = \frac{\pi}{2} J_c |\sin q_c| \quad \& \quad E_u(q_c) = \pi J_c \left| \sin \frac{q_c}{2} \right|,$$

where q_c is the projected wave vector along the c -axis in the unit of *r.l.u.*, and J_c is the AFM superexchange interaction. As a good approximation, the magnetic dynamic structure factor at $T=0$ K can be expressed as [34]:

$$S(E, q) = \frac{289.6}{\pi} \frac{H[E - E_l(q)] \times H[E_u(q) - E]}{\sqrt{E^2 - E_l(q)^2}},$$

here, $H[x]$ is the Heaviside step function. We evaluated this expression using $J_c = 34$ meV which is based on the INS results [33]. Before we plot the calculated spectra, it is noteworthy that the photon momentum transfer along the sample c -axis passes through the AFM wavevector $q_c = 0.5$ *r.l.u.* twice under the fixed RIXS scattering configuration [26]. Correspondingly, we show theoretical results as a function of q_c in Fig.4 (c) [26]. In Fig.4 (a) and (b), we plot the momentum transfer q_c at the bottom axes and superimposed the two-spinon continuum lower and upper boundaries (white dashed lines) on top of the experimental results. Remarkably, the centre of mass of RIXS low-energy excitations match extremely well with the lower limit of two-spinon dispersions. In particular, two maximal intensity spots near the zero loss energy position agree precisely with the theoretical results which reach minimal dispersion.

Comparing RIXS results with INS data [33], some extra spectral weight seems to exist specifically near $q_c = 0.5$ *r.l.u.* We plot the corresponding line spectra in Fig.4

(d) together with the theoretical result. The peak position of the mode appears at ~ 40 (47) meV for σ (π) polarizations which is absent in the theory. The longitudinal magnetic mode, *i.e.*, the signature of the 3D magnetic ordering, should in principle exist in RIXS spectra as the experiments were conducted below T_N of 38 K [35]. However, its centre energy of ~ 18.5 meV is below the RIXS energy resolution. On the other hand, the mode seems to be comparable to the optical phonon observed by Raman [36] and IXS [32]. To further explore the origin of the mode, we performed temperature-dependent measurements at $q_c=0.5$ *r.l.u.* and the data are shown in Fig.4 (e). The persistence of the peak up to room temperature in both polarizations demonstrate its phonon-like origin.

We are now ready to address the main question of the paper, which is related to the onset of the orbiton dispersion in KCuF_3 . Aided by the ab initio QC calculation, we confirm that the orbital excitation in the KCuF_3 RIXS spectra are dominated by the localized *dd* excitations. Moreover, a very good agreement between the RIXS spectra and the Muller Ansatz calculations demonstrates that the orbiton dispersion must be well below the nicely observed dispersion of the spinons, which is governed by the spin exchange $J_c = 34$ meV. Whereas, taking into account *solely* the superexchange mechanism the orbital exchange well below that order of magnitude cannot be ruled out, the following puzzle remains: Why the large Jahn-Teller coupling (~ 70 meV, as inferred from $T_{OO} \sim 800$ K) does not lead to a sizeable and observable orbiton dispersion. While we leave a detailed answer to this question for a future work, we here suggest the following explanation. Apart from the cooperative, global Jahn-Teller effect and ordering, the *local* Jahn-Teller effect, *i.e.* the Jahn-Teller coupling between the orbital degrees of freedom and the *local* lattice vibrations is of prime importance [20, 37]. As discussed in Ref. [20], the latter effect, which should be present in any Jahn-Teller active system, can lead to a strong dressing of the orbitons with local vibrational modes and may cause a complete smearing out of the orbiton dispersion, cf. Fig. 5(b) of [20]. Since the Jahn-

Teller coupling is inherently strong in KCuF_3 we believe this scenario explains the effective disappearance of the orbiton dispersion in this compound.

IV. CONCLUSION

In summary, we performed high-resolution RIXS experiments on the orbitally-ordered KCuF_3 . The high-energy excitations are found to stem from localized dd orbital excitations, consistent with the *ab-initio* calculation based on a single cluster. The low-energy dispersive excitations are dominated by the two-spinon continuum via the comparison to Mueller Ansatz calculations. This indicates that the relevant energy bandwidth of the orbitons may be much lower than the energy resolution (corresponding to a half maximum of 37 meV) of RIXS experiments. We suggest that the main reason for the lack of the onset of an orbiton with a dispersion above the resolution threshold lies in the possibly strong local Jahn-Teller effect, which may lead to the dressing of the orbiton with the local vibrational modes and thus to the suppression of the orbiton dispersion.

V. ACKNOWLEDGEMENTS

We thank E. Pavarini for fruitful discussions. We also thank Nikolay Bogdanov for the assistance on the theo-

retical models. J.L. acknowledges Diamond Light Source (United Kingdom) and the Institute of Physics in Chinese Academy of Sciences (China) for providing funding Grant 112111KYSB20170059 for the joint Doctoral Training under the contract STU0171, and also the financial support from China Scholarship Council. L.X. thanks U. Nitzsche for technical assistance. JSZ acknowledges the support by NSF Grant No. DMR-1905598 in USA. K.W. acknowledges support by Narodowe Centrum Nauki (NCN) Project No. 2016/22/E/ST3/00560. JvdB acknowledges financial support through the Deutsche Forschungsgemeinschaft (DFG, German Research Foundation), SFB 1143 project A5 and through the Würzburg-Dresden Cluster of Excellence on Complexity and Topology in Quantum Matter - ct.qmat (EXC 2147, project-id 39085490). H.D. acknowledges support by the National Natural Science Foundation of China (No.11888101) and the Ministry of Science and Technology of China (2016YFA0401000). All data were taken at the I21 RIXS beamline of Diamond Light Source (United Kingdom) using the RIXS spectrometer designed, built and owned by Diamond Light Source. We acknowledge Diamond Light Source for providing the science commissioning time on Beamline I21. We acknowledge Thomas Rice for the technical support throughout the beamtime. We would also like to thank the Materials Characterisation Laboratory team for help on the Laue instrument in the Materials Characterisation Laboratory at the ISIS Neutron and Muon Source.

-
- [1] Y. Tokura and N. Nagaosa, *Science* **288**, 462 (2000).
 - [2] C. D. Ling, J. E. Millburn, J. F. Mitchell, D. N. Argyriou, J. Linton, and H. N. Bordallo, *Phys. Rev. B* **62**, 15096 (2000)
 - [3] Y. Ren, T. T. M. Palstra, D. I. Khomskii, E. Pellegrin, A. A. Nugroho, A. A. Menovsky and G. A. Sawatzky, *Nature* **396**, 441–444(1998).
 - [4] M. T. Hutchings, E. J. Samuelsen, G. Shirane, and K. Hirakawa, *Phys. Rev.* **188**, 919 (1969).
 - [5] R. Caciuffo, L. Paolasini, A. Sollier, P. Ghigna, E. Pavarini, J. van den Brink, and M. Altarelli, *Phys. Rev. B* **65**, 174425 (2002).
 - [6] L. Paolasini, R. Caciuffo, A. Sollier, P. Ghigna, and M. Altarelli, *Phys. Rev. Lett.* **88**, 106403 (2002).
 - [7] S. K. Satija, J. D. Axe, G. Shirane, H. Yoshizawa, and K. Hirakawa, *Phys. Rev. B* **21**, 2001 (1980).
 - [8] E. Pavarini, E. Koch and A. I. Lichtenstein, *Phys. Rev. Lett.* **101**, 266405 (2008).
 - [9] K. I. Kugel and D. I. Khomskii, *Soviet Physics Uspekhi*. **25**, 231 (1982).
 - [10] J. van den Brink, P. Horsch, F. Mack, and A. M. Oleś, *Phys. Rev. B* **59**, 6795 (1999).
 - [11] E. Saitoh, S. Okamoto, K. T. Takahashi, K. Tobe, K. Yamamoto, T. Kimura, S. Ishihara, S. Maekawa and Y. Tokura, *Nature (London)* **410**, 180 (2001).
 - [12] M. Grüninger, R. Rückamp, M. Windt, P. Reutler, C. Zobel, T. Lorenz, A. Freimuth, A. Revcolevschi, *Nature (London)* **418**, 39 (2002).
 - [13] J. Schlappa, K. Wohlfeld, K. J. Zhou, M. Mourigal, M. W. Haverkort, V. N. Strocov, L. Hozoi, C. Monney, S. Nishimoto, S. Singh, A. Revcolevschi, J. S. Caux, L. Patthey, H. M. Ronnow, J. van den Brink, and T. Schmitt, *Nature (London)* **485**, 82 (2012).
 - [14] V. Bisogni, K. Wohlfeld, S. Nishimoto, C. Monney, J. Trinckauf, K. Zhou, R. Kraus, K. Koepf, C. Sekar, V. Strocov, B. Büchner, T. Schmitt, J. van den Brink, and J. Geck, *Phys. Rev. Lett.* **114**, 096402 (2015).
 - [15] R. Fumagalli, J. Heverhagen, D. Betto, R. Arpaia, M. Rossi, D. Di Castro, N. B. Brookes, M. Moretti Sala, M. Daghofer, L. Braicovich, K. Wohlfeld, and G. Ghiringhelli, *Phys. Rev. B* **101**, 205117 (2020).
 - [16] K. Wohlfeld, M. Daghofer, S. Nishimoto, G. Khaliullin, and J. van den Brink, *Phys. Rev. Lett.* **107**, 147201 (2011).
 - [17] K. Wohlfeld, S. Nishimoto, M. W. Haverkort, and J. van den Brink, *Phys. Rev. B* **88**, 195138 (2013).
 - [18] S. Okamoto, S. Ishihara, and S. Maekawa, *Phys. Rev. B* **66**, 014435 (2002).
 - [19] J. van den Brink, *New J. Phys.* **6**, 201 (2004).
 - [20] J. Nasu and S. Ishihara, *Phys. Rev. B* **88** 205110 (2013).
 - [21] M. Moretti Sala, V. Bisogni, C. Aruta, G. Balestrino, H. Berger, N. B. Brookes, G. M. de Luca, D. Di Castro, M. Grioni, M. Guarise, P. G. Medaglia, F. Miletto Granozio, M. Minola, P. Perna, M. Radovic, M. Salluzzo, T. Schmitt, K. J. Zhou, L. Braicovich, and G. Ghiringhelli, *New J. Phys.* **13**, 043026 (2011).

- [22] Luuk J. P. Ament, Michel van Veenendaal, Thomas P. Devereaux, John P. Hill, and Jeroen van den Brink, *Rev. Mod. Phys.* **83**, 705 (2011).
- [23] L. Braicovich, J. van den Brink, V. Bisogni, M.M. Sala, L.J.P. Ament, N.B. Brookes, G.M. De Luca, M. Salluzzo, T. Schmitt, V.N. Strocov, and G. Ghiringhelli, *Phys. Rev. Lett.* **104**, 077002 (2010).
- [24] C. Ulrich, G. Ghiringhelli, A. Piazzalunga, L. Braicovich, N. B. Brookes, H. Roth, T. Lorenz, and B. Keimer, *Phys. Rev. B* **77**, 113102 (2008).
- [25] L. G. Marshall, J. Zhou, J. Zhang, J. Han, S. C. Vogel, Y. Zhao, M. T. Fernandez-Diaz, X. Yu, J. Cheng, and J. B. Goodenough, *Phys. Rev. B* **87**, 014109 (2013).
- [26] Supplementary materials are available online XXXX.
- [27] C. De Nadai, A. Demourgues, and J. Grannec, F. M. F. de Groot, *Phys. Rev. B* **63**, 125123 (2001).
- [28] M. Hidaka, T. Eguchi, and I. Yamada, *J. Phys. Soc. Jpn.* **67**, 2488 (1998).
- [29] J. Deisenhofer, I. Leonov, M. V. Eremin, Ch. Kant, P. Ghigna, F. Mayr, V. V. Iglamov, V. I. Anisimov, and D. van der Marel, *Phys. Rev. Lett.* **101**, 157406 (2008).
- [30] K. Ishii, S. Ishihara, Y. Murakami, K. Ikeuchi, K. Kuzushita, T. Inami, K. Ohwada, M. Yoshida, I. Jarrige, N. Tatami, S. Niioka, D. Bizen, Y. Ando, J. Mizuki, S. Maekawa, and Y. Endoh, *Phys. Rev. B* **83**, 241101(R) (2011).
- [31] T. Helgaker, P. Jorgensen and J. Olsen, *Molecular Electronic-Structure Theory* (Wiley, Chichester, 2000).
- [32] Y. Tanaka, A. Q. R. Baron, Y.-J. Kim, K. J. Thomas, J. P. Hill, Z. Honda, F. Iga, S. Tsutsui, D. Ishikawa, and C. S. Nelson, *New J. Phys.* **6**, 161 (2004).
- [33] B. Lake, D. A. Tennant, C. D. Frost, and S. E. Nagler, *Nat. Mater.* **4**, 329 (2005).
- [34] G. Muller, H. Thomas, H. Beck, and J. C. Bonner, *Phys. Rev. B* **24**, 1429 (1981).
- [35] B. Lake, D. A. Tennant, and S. E. Nagler, *Phys. Rev. B* **71**, 134412 (2005).
- [36] J.C.T. Lee *et al.*, *Nat. Phys.* **8**, 63 (2012).
- [37] J. van den Brink, *Phys. Rev. Lett.* **87**, 217202 (2001).